Development 137, 3625-3632 (2010) doi:10.1242/dev.054452

Notch signalling regulates left-right asymmetry through ciliary length control

Susana S. Lopes[1,2], Raquel Lourenço[1,2], Luís Pacheco[2], Nuno Moreno[2], Jill Kreiling[3] and Leonor Saúde[1,2,*]

SUMMARY

The importance of cilia in embryonic development and adult physiology is emphasized by human ciliopathies. Despite its relevance, molecular signalling pathways behind cilia formation are poorly understood. We show that Notch signalling is a key pathway for cilia length control. In *deltaD* zebrafish mutants, cilia length is reduced in Kupffer´s vesicle and can be rescued by the ciliogenic factor *foxj1a*. Conversely, cilia length increases when Notch signalling is hyperactivated. Short cilia found in *deltaD* mutants reduce the fluid flow velocity inside Kupffer´s vesicle, thus compromising the asymmetric expression of the flow sensor *charon.* Notch signalling brings together ciliary length control and fluid flow hydrodynamics with transcriptional activation of laterality genes. In addition, our *deltaD* mutant analysis discloses an uncoupling between gut and heart laterality.

KEY WORDS: Notch, Cilia, Left-right, Zebrafish

INTRODUCTION

Internal body left-right (LR) asymmetry is a common trait among vertebrates. In contrast to the symmetric external body plan, the heart, digestive organs and parts of the brain display highly conserved asymmetric orientations that are essential for their correct functions. When the normal asymmetric distribution of the internal organs is compromised, human laterality disorders arise such as heterotaxy and situs inversus (Fliegauf et al., 2007; Gerdes et al., 2009).

The establishment of LR asymmetries in vertebrates occurs during early stages of embryonic development through a complex process involving epigenetic and genetic mechanisms. This culminates in the activation of a conserved Nodal signalling cascade that starts at the node and is then transferred to the left lateral plate mesoderm (LPM) (Hamada, 2008). Although the timing and mechanism responsible for breaking the initial embryonic symmetry might differ between species, it is clear that a directional fluid flow generated by motile cilia present in the node plays a fundamental role in LR determination, most likely by creating a LR information bias in the node (Levin and Palmer, 2007). Several lines of evidence support this idea, namely absent cilia in the mouse (Nonaka et al., 1998), shorter cilia in zebrafish mutants and morphants (Kramer-Zucker et al., 2005; Neugebauer et al., 2009), and immotile cilia in mouse, zebrafish and medaka (Essner et al., 2005; Hojo et al., 2007; Supp et al., 1999). All these cilia defects result in altered fluid flow in the node/Kupffer's vesicle (KV) and ultimately in LR defects. This implies that proper cilia length regulation is crucial for the establishment of LR asymmetries.

[1]Instituto de Medicina Molecular e Instituto de Histologia e Biologia do Desenvolvimento, Faculdade de Medicina da Universidade de Lisboa, 1649-028 Lisboa, Portugal. [2]Instituto Gulbenkian de Ciência, P-2780-156 Oeiras, Portugal. [3]Department of Molecular Biology, Cell Biology, and Biochemistry, Brown University, Providence, RI 02912, USA.

*Author for correspondence (msaude@fm.ul.pt)

Accepted 25 August 2010

Expression of *Nodal* and of its antagonist *Cerl2* (*Dand5* – Mouse Genome Informatics) in the mouse node starts symmetrically (Collignon et al., 1996; Marques et al., 2004). However, the mechanism that produces asymmetrical expression of *Nodal* and *Cerl2* on the left and right sides of the node, and its potential link to the leftward nodal flow, is not fully understood. In zebrafish, there is no evidence for asymmetric expression of *spaw* and of its negative regulator *charon* in KV. Nevertheless, it has been suggested that an asymmetric Charon function inhibits the transfer of *spaw* to the right LPM (Hashimoto et al., 2004). To date, the relationship between the fluid flow inside KV and the asymmetric function of Charon in medaka and its homologue Coco in *Xenopus* have been studied (Hojo et al., 2007; Schweickert et al., 2010), but this relationship has not been explored in zebrafish.

Notch signalling has been implicated in LR patterning in vertebrates, largely through the activation of *Nodal* expression in the murine node (Krebs et al., 2003; Przemeck et al., 2003; Raya et al., 2003; Takeuchi et al., 2007). In zebrafish, Notch signalling seems to activate *charon* expression in KV (Gourronc et al., 2007).

Apart from providing the first genetic evidence in zebrafish for the activation of *charon* expression in KV, we demonstrate that canonical Notch signalling, through the DeltaD ligand, is a key regulator of ciliary length at the KV. We show that reduction of Notch signalling produces shorter cilia, whereas hyperactivation of Notch produces longer cilia; thus, providing new insights into how cilia length is modulated. We find that the correct regulation of cilia length has a strong impact on the directionality and speed of fluid flow inside KV, and we were able to show that this biomechanical event correlates with asymmetric transcription of *charon*. Altogether, our results reveal a new and multistep role for the Notch signalling pathway that couples two fundamental processes in left-right determination: transcription of *charon* and ciliary length regulation that then culminates in breaking the symmetry of *charon* expression.

MATERIALS AND METHODS

Zebrafish line

AB wild type and mutant (*notch1a*/*des*^{Tp37}, *deltaC*/*bea*^{tit446}, *deltaD*/*aei*^{tr233}) embryos were staged according to Kimmel et al. (Kimmel et al., 1995).

Morpholino antisense oligo (MO) and mRNA microinjections

deltaD-MO as described previously (Holley et al., 2000) was injected from 0.5-1.0 mM into 512-cell stage wild-type embryos. The MO that blocks translation of *Su(H)1* and *Su(H)2* was used as previously described (Echeverri and Oates, 2007). Notch-intracellular and full-length *deltaD* constructs (Takke and Campos-Ortega, 1999; Takke et al., 1999) were injected at the one-cell stage at a concentration of 100 pg and 350 pg, respectively. *foxj1a* and GFP full-length cDNAs were independently cloned into pCS2^{+} and in vitro transcribed using mMESSAGE mMACHINE kit (Ambion). The *foxj1a* and GFP mRNAs were injected at a concentration of 100 pg. Embryos were left to develop at 28°C until the desired stage and then fixed in 4% PFA at 4°C overnight.

In situ hybridization

Whole-mount in situ hybridization was performed as described previously (Thisse and Thisse, 2008). Digoxigenin RNA probes were synthesized from DNA templates of *spaw* (Hashimoto et al., 2004), *pitx2* (Essner et al., 2005), *lefty2* (Bisgrove et al., 2005), *foxa3* (Monteiro et al., 2008), *ntl* (Amack and Yost, 2004), *shh* (Essner et al., 2005), *charon* (Hashimoto et al., 2004), *deltaD* (Takke and Campos-Ortega, 1999), *sox17* (Amack and Yost, 2004) and *foxj1a* (Neugebauer et al., 2009; Yu et al., 2008).

Antibody staining and immunofluorescence

We followed the methods described previously (Neugebauer et al., 2009) for immunostaining. In some cases, we also used TOPRO-3 (1:1000; Invitrogen) diluted in blocking solution.

Confocal microscopy

Flat-mounted embryos were examined with a Zeiss LSM 510 Meta confocal microscope. Three-colour confocal *z*-series images were acquired using sequential laser excitation, converted into a single plane projection and analyzed using ImageJ software (LSM Reader). The length of all cilia in each KV was measured using ImageJ Segmented Line Tool.

High-speed video microscopy

We used the confocal microscope Leica SP5 under the resonance mode, which allows imaging at 8000 lines per second, to acquire images of ciliary beating and debris movements inside KV of live embryos mounted in 1% low-melting agarose (Sigma). High-speed films of the debris were analyzed using ImageJ and the velocity was measured by tracing the debris frame by frame. The orientation and speed of the debris were calculated using Excel VBA, and vectors were drawn using the Gnuplot software and Gimp.

Determination of KV cilia distribution

The total number of cilia and their distribution within KV were determined from confocal *z*-stacks as previously described (Kreiling et al. 2007).

RESULTS

DeltaD is the Notch ligand that defines laterality in zebrafish

In order to study the impact of Notch signalling pathway on crucial steps for LR patterning, we used several mutants and reagents. We started by evaluating the asymmetric information in the LPM using the left-identity molecular markers *spaw* and *pitx2*. The *nodal*-related gene *spaw* is the earliest molecule to be asymmetrically detected in the left LPM and is known to induce the expression of the transcription factor *pitx2* (Hamada et al., 2002; Long et al., 2003).

We show that mutants in the Notch transmembrane receptor, *des/notch1a*$^{-/-}$, lose their laterality identity by becoming largely bilateral (Fig. 1A,B). Upon binding to its ligand, the intracellular domain of Notch (NICD) is cleaved and translocates into the nucleus. In the nucleus, NICD binds to Suppressor-of-Hairless [Su(H)] thereby changing its repressor status to an activator (Fior and Henrique, 2009). In zebrafish, two *Su(H)* gene paralogs (*rbpja* and *rbpjb* – Zebrafish Information Network) can be knocked down using a single antisense morpholino that blocks the translation of both [*Su(H)1+2-MO*] (Echeverri and Oates, 2007). Consistent with our results, *Su(H)1+2* morphants also showed lack of laterality identity (Fig. 1A,B). To directly induce the Notch pathway, we injected the mRNA encoding NICD and, similar to what has been described previously (Raya et al., 2003), we again found a loss in laterality (Fig. 1A,B). These results indicate that canonical Notch signalling is required to define laterality in the LPM.

In order to assess which Notch ligand was the most relevant in LR establishment, the expression of the left-sided markers was analysed in the null mutants *aei/deltaD*$^{-/-}$ and *bea/deltaC*$^{-/-}$. In clear contrast to *bea*$^{-/-}$, *aei*$^{-/-}$ mutants have a strong *pitx2* laterality phenotype that can be rescued by NICD (Fig. 1B). Thus, we identified DeltaD as the key Notch ligand for LR asymmetry in zebrafish and we focus our analysis on this null mutant. We find that the bilateral expression of *pitx2* does not always follow the expression of *spaw* (compare Fig. 1A with 1B). A lack of a precise correlation between the expression of *nodal* and *pitx2* in the LPM was already described in the context of delta-like 1 (*Dll1*) mouse mutants (Krebs et al., 2003; Przemeck et al., 2003; Raya et al., 2003). Altogether, these results show that Notch signalling regulates *pitx2* expression in a Nodal/Spaw independent manner.

The axial midline is required to maintain LR asymmetry by acting as a midline barrier (Chin et al., 2000; Hamada et al., 2002). We checked whether the LR defects that arise upon Notch signalling perturbation were due to lack of a midline. We found that the expression pattern of both *shh* and *ntl* markers was normal in all the experimental conditions (see Fig. S1A-N in the supplementary material), with the exception of *ntl* downregulation in NICD-injected embryos (see Fig. S1N in the supplementary material), in agreement with what has been described previously (Latimer and Appel, 2006). Therefore, LR defects arising from reduced Notch signalling are not likely to be due to an absent midline.

DeltaD maintains *spaw* expression in the posterior left LPM

In *aei*$^{-/-}$ mutants, *spaw* expression is only mildly randomized (Fig. 1A), but the expression scored as being left-sided (Fig. 1A) shows three distinct patterns that have been quantified in detail in Fig. 1C. Namely, we could detect *spaw* expression in a left anterior domain (Fig. 1C,D,D′), in a left anterior and posterior domains (Fig. 1C,F,F′), and in a left anterior domain with bilateral posterior domains with competition (Fig. 1C,G). Although, a posterior downregulation of *spaw* occurs at the 23-somite stage as part of its normal anteroposterior (AP) expression pattern (Long et al., 2003), our analysis using an *aei* heterozygous cross, clearly shows that this *spaw* downregulation occurs prematurely at the 16-somite stage in 67% of the homozygous embryos (Fig. 1C,D,D′). In agreement with this posterior downregulation of *spaw*, we observe that *lefty1*, which is known to be induced by Spaw (Long et al., 2003; Wang and Yost, 2008), has also an abnormal expression gap in the corresponding midline domain (Fig. 1E). These results suggest that the maintenance of *spaw* expression in the posterior left LPM and possibly *lefty1* in the midline domain require DeltaD function.

DeltaD controls gut laterality

Next, we evaluated the impact that the abnormal expression of *spaw* and *pitx2* seen in *aei*$^{-/-}$ mutants has on heart and gut positioning. We scored *aei*$^{-/-}$ mutants for heart asymmetry in vivo and made use of the prospective heart marker *lefty2* and of the gut marker *foxa3* in fixed embryos. We show that in *aei*$^{-/-}$ mutants, gut

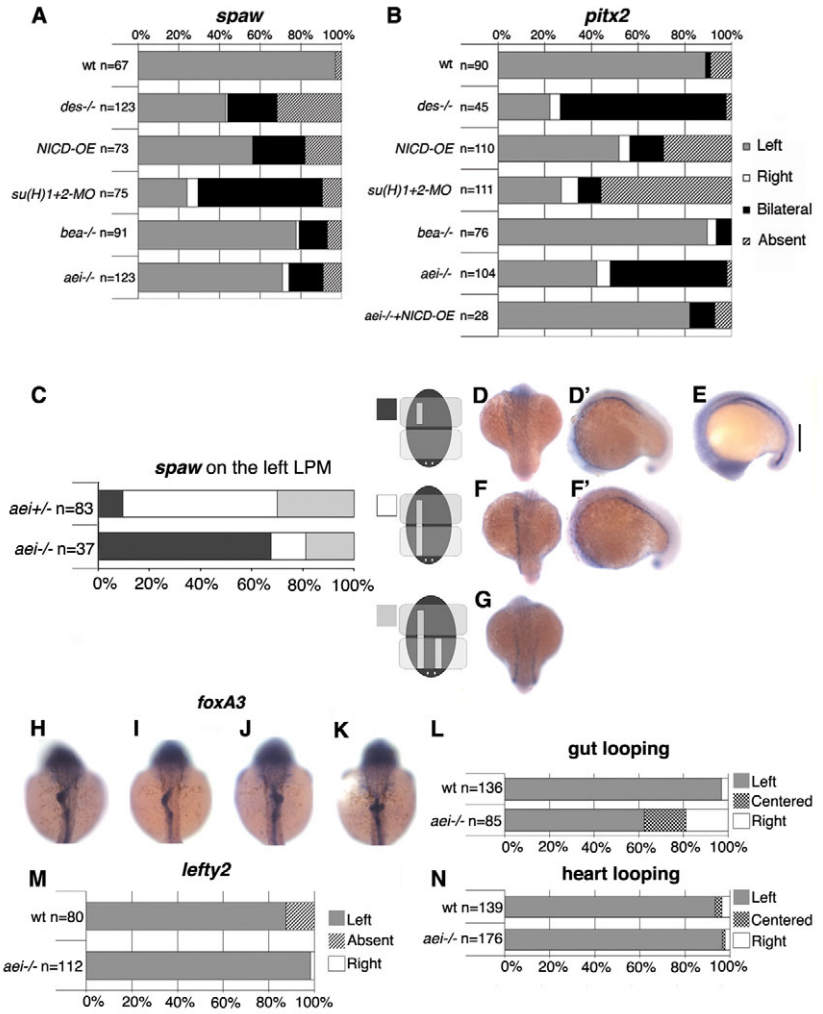

Fig. 1. Canonical Notch signalling through the DeltaD ligand controls left-right patterning. (**A**,**B**) Percentages of normal (Left, grey), reversed (Right, white), bilateral (black) and absent (stripes) expression of *spaw* (A) and *pitx2* (B) in the lateral plate mesoderm when Notch signalling was challenged. Embryos were analysed between the 14- and 18-somite stages for *spaw* expression and between the 18- and 20-somite stages for *pitx2*. (**C**) Percentages of different domains of left-sided expression of *spaw* in the lateral plate mesoderm. (**D**,**D′**,**F**,**F′**,**G**) In *aei*$^{-/-}$ embryos, *spaw* may be expressed in an anterior domain only (D,D′), in an anterior with bilateral posterior domains (F,F′), and in anterior and posterior domains with competition on the right side (G). (**E**) A double *spaw* and *lefty1* in situ hybridization showing the posterior gap (vertical line) of these two markers in an *aei*$^{-/-}$ embryo. (**H-K**) Expression of *foxa3* in the gut in 50-53 hpf embryos (dorsal views). In wild-type embryos, the gut loops to the left (H). In *aei*$^{-/-}$ embryos, the gut may loop to the left (I), or to the right (J), or show no looping (K). (**L**) Percentages of normal (Left), reversed (Right) or no looping of the gut at 50-53 hpf. (**M**) Percentages of normal (Left), reversed (Right) or absent *lefty2* in the lateral plate mesoderm at the 26-somite stage. (**N**) Percentages of normal (Left), reversed (Right) or no jogging (Centered) of the heart at 30-32 hpf.

looping is randomized (62.3% loops to the left, 18.8% failed loops and 18.8% loops to the right; *n*=85) (Fig. 1H-L). By contrast, heart jogging is not significantly affected when evaluated by *lefty2* expression at 26-somite stage (99% on the left; *n*=112) or when judged by direct observation at 30 hpf (90.7% on the left; *n*=65) (Fig. 1M,N). These results indicate the uncoupling of laterality of an anterior organ, such as the heart, and of more posterior organs, such as the liver and pancreas. The heart is the first organ to be asymmetrically positioned in zebrafish, and it seems that its asymmetry may arise by a mechanism different from that governing other viscera, as suggested by others (Chin et al., 2000; Lin and Xu, 2009).

Our data indicate that the prospective heart domain is unaffected in the *aei*$^{-/-}$ mutants and thus provide an explanation for why heart laterality is not disturbed. Namely, the anterior left-sided LPM expression of *spaw* is unaffected and *pitx2* does not reach the anterior-most domain when expressed on the right LPM. We propose that the premature absence of *spaw* expression in the posterior LPM, coupled with a bilateral *pitx2* expression in this region could underlie the gut laterality phenotype observed in 40% of *aei*$^{-/-}$ mutants.

DeltaD regulates cilia length in KV

Increasing evidence shows that a properly formed node/KV with a directional strong fluid flow driven by the beating of motile cilia is essential for LR determination (Amack et al., 2007; Hamada, 2008). We therefore investigated whether the laterality problems observed in *aei*$^{-/-}$ mutants were due to KV morphogenesis and/or ciliogenesis defects.

To test KV integrity, we performed immunostaining with ZO-1, a tight junction marker and aPKC an apical epithelial marker (Neugebauer et al., 2009) and observed live embryos with high resolution DIC microscopy. The three approaches revealed that KV structure is normal both in *aei*$^{-/-}$ mutants and in *deltaD* overexpressing embryos (Fig. 2A-I). We thus conclude that KV morphogenesis and polarity are not affected by downregulation or upregulation of Notch signalling.

To investigate the role of DeltaD in cilia formation, we labelled the KV cilia with an anti-acetylated α-tubulin antibody. We found that cilia length is significantly reduced in *aei*$^{-/-}$ mutants [Fig. 2J,K,M; 2.25±0.62 μm (s.d.m.); *n*=20 embryos; $P<4.3\times10^{-9}$) when compared with cilia length in wild-type embryos (Fig. 2J,K,L; 3.73±0.76 μm (s.d.m.); *n*=27 embryos). Strikingly, we also found that hyperactivation of Notch signalling significantly increased the length of cilia in KV either by injection of NICD [Fig. 2J; 5.28±1.23 μm (s.d.m.); *n*=19 embryos; $P<3.5\times10^{4}$] or *deltaD* [Fig. 2J,K,N; 6.78±1.18 μm (s.d.m.); *n*=11 embryos; $P<1.5\times10^{-4}$]. Additionally, we asked whether cilia motility was also affected in *aei*$^{-/-}$ mutants. We filmed the KV cilia in live *aei*$^{-/-}$ embryos and showed that, despite being shorter, cilia are still motile (see Movie 2 in the supplementary material). These results strongly suggest that Notch signalling, through DeltaD, controls ciliary length in KV.

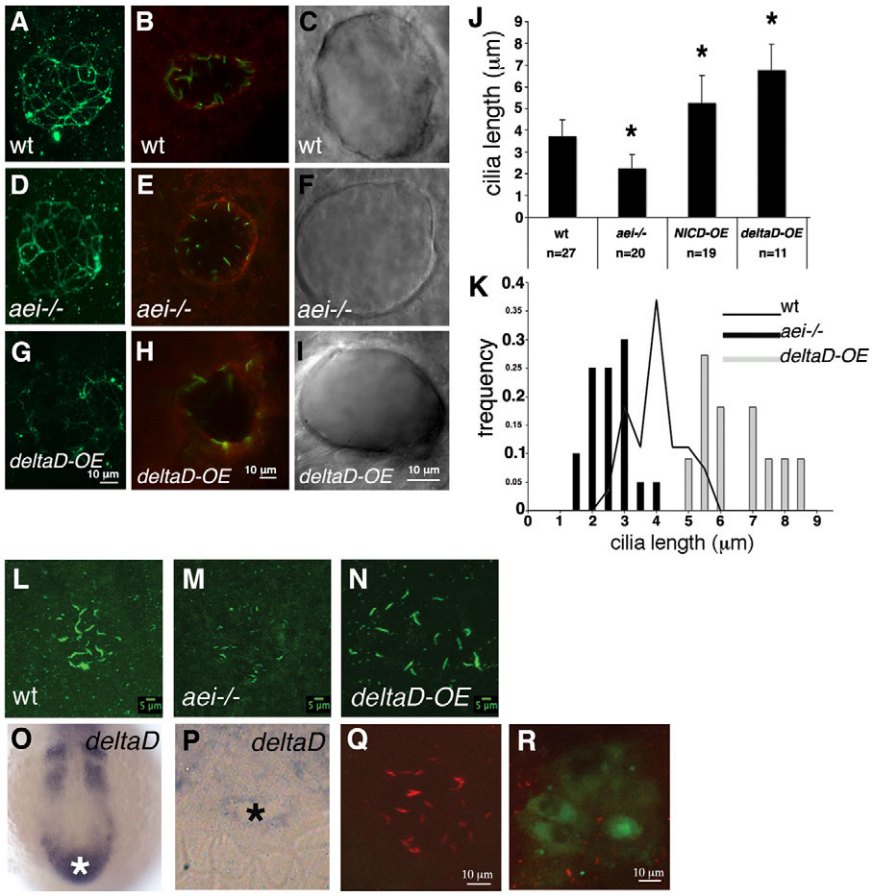

Fig. 2. DeltaD regulates cilia length in the Kupffer's vesicle. (**A**,**D**,**G**) ZO-1 immunostaining of a representative wild-type embryo (A), an *aei*$^{-/-}$ mutant embryo (D) and a *deltaD*-overexpressing embryo (G). (**B**,**E**,**H**) aPKC immunostaining of a representative wild-type embryo (B), an *aei*$^{-/-}$ mutant embryo (E) and a *deltaD*-overexpressing embryo (H). (**C**,**F**,**I**) DIC images of live embryos showing a wild-type KV (C), a KV from an *aei*$^{-/-}$ embryo (F) and a KV from a *deltaD*-overexpressing embryo (I). (**J**) Quantification of ciliary length at 10-somite stages in wild type, in *aei*$^{-/-}$ mutants and in embryos where Notch signalling was hyperactivated by overexpressing NICD (*NICD-OE*) or *deltaD* (*deltaD-OE*). Asterisks indicate experimental conditions that produce changes that are significantly different from wild type ($P<0.001$, Student's *t*-test, two tail for two samples assuming unequal variances). (**K**) Histogram showing the distribution of Kupffer´s vesicle ciliary length at 10-somite stages in *aei*$^{-/-}$ mutant embryos (black bars), wild-type embryos (black line) and embryos subjected to *deltaD-OE* (grey bars). (**L-N**) Confocal images of all *z*-sections spaced 1 μm apart through the entire ciliated Kupffer´s vesicle at the 10-somite stage. Cilia are labelled with anti-acetylated α-tubulin in a wild-type embryo (L), an *aei*$^{-/-}$ mutant (M) and an embryo subjected to *deltaD-OE* (N). (**O**,**P**) Wild-type *deltaD* expression at the 10-somite stage in whole mount (O) and in resin section (P). The white and the black asterisks label the position and the lumen of the Kupffer´s vesicle, respectively. (**Q**,**R**) *deltaD*-MO co-injected with fluorescein lineage tracer in the dorsal forerunner cells (DFCs). (Q) Injected embryo with non-targeted Kupffer´s vesicle cells showing normal length cilia. (R) Fluorescein-positive Kupffer´s vesicle cells with shorter cilia. Error bars indicate s.d.m.

deltaD is expressed in the KV (Fig. 2O,P) and also in its precursors at the bud stage (10 hpf), in the somites, presomitic mesoderm and tail bud throughout segmentation stages (Hsiao et al., 2007). Therefore, we decided to test whether the short cilia phenotype observed in *aei*$^{-/-}$ mutants is caused by the lack of DeltaD function specifically in the KV precursors or in KV cells. We targeted the dorsal forerunner cells (DFC), which are the KV precursors (Essner et al., 2005), by co-injecting the lineage tracer fluorescein and a *deltaD*-MO at the midblastula stage. In KV cells where fluorescein (and therefore *deltaD*-MO) was successfully detected, we observed a reduction in cilia length comparable with the one quantified in *aei*$^{-/-}$ mutants [Fig. 2R; 2.25 ±0.6 μm (s.d.m.); $n=29$ cells; $P=0.3$) and different from the one quantified in KV cells that were not successfully targeted [Fig. 2Q; 3.6±0.6 μm (s.d.m.); $n=21$ cells; $P<1.6\times10^{-7}$]. This experiment indicates that DeltaD autonomously regulates cilia length at the level of the KV precursors or the KV cells and not in the somites, presomitic mesoderm and tail bud. In agreement, we found that in embryos where KV precursors were successfully targeted with *deltaD*-MO the trend in *spaw* (84% on the left; 7% on the right; 8% bilateral; $n=57$) and *pitx2* (33% on the left; 41% bilateral; 25% absent; $n=12$) expression is similar to the one observed in *aei*$^{-/-}$ mutants. Moreover, embryos injected with *deltaD*-MO at the midblastula stage, showed gut looping defects (74% loops to the left, 18% does not loop and 8% loops to the right; $n=123$) and had no heart laterality problems similar to what we described for the *aei*$^{-/-}$ mutants.

DeltaD maintains proper cilia length through modulation of *foxj1a*

In order to investigate why the *aei*$^{-/-}$ mutant cilia are shorter, we analysed the expression pattern of *foxj1a*, a marker of KV motile cilia (Amack and Yost, 2004; Stubbs et al., 2008; Yu et al., 2008). At the bud stage, the DFC marker *sox17* was detected in both *aei*$^{-/-}$

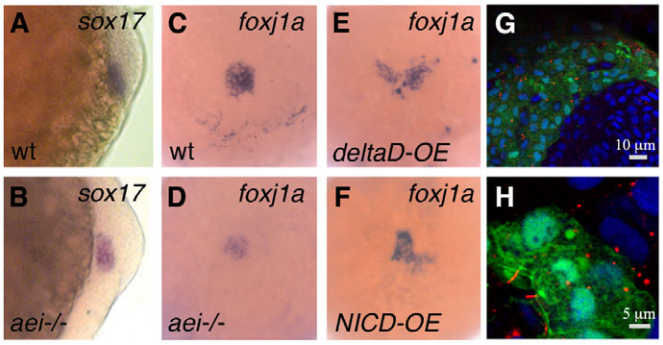

Fig. 3. DeltaD modulates *foxj1a* expression. (**A**,**B**) Expression pattern of *sox17* in Kupffer's vesicle precursor cells at bud stage in wild-type (A) and *aei*$^{-/-}$ mutant (B) embryos. (**C-F**) Expression pattern of *foxj1a* in Kupffer's vesicle precursor cells at bud stage in a wild-type (C), an *aei*$^{-/-}$ mutant (D), a wild type overexpressing *deltaD* and a wild type overexpressing NICD (F). (**G**,**H**) Foxj1a mRNA injection increases ciliary length. (G) Tail region of an *aei*$^{-/-}$ mutant embryo showing GFP-positive cells that were co-targeted with *foxj1a* and GFP mRNA. In these cells, cilia are much larger than in adjacent non-targeted cells. (H) Cells from the Kupffer's vesicle in an *aei*$^{-/-}$ mutant embryo that was co-injected with *foxj1a* and GFP mRNA showing rescued motile cilia judged by the increased ciliary length. α-Acetylated tubulin labels cilia in red, DAPI labels DNA in blue and GFP labels targeted cells in green.

and wild-type embryos (Fig. 3A,B), confirming presence of DFCs. By contrast, *foxj1a* expression was downregulated in *aei*$^{-/-}$ mutants at the same stage compared with wild-type embryos (Fig. 3C,D). We further confirmed that *foxj1a* expression was downregulated at bud stages in 25% of the embryos that resulted from an *aei* heterozygous cross (n=157). In addition, overexpression of both *deltaD* and *NICD* mRNA resulted in ectopic expression of *foxj1a* in the DFCs region at the bud stage (Fig. 3E,F). We thus propose that DeltaD controls KV cilia length via the regulation of *foxj1a*. Consistently, *foxj1a* morphants also show shorter or absent cilia in the KV (Stubbs et al., 2008; Yu et al., 2008).

In order to test whether Notch signalling is working via Foxj1a, we performed an epistatic test by co-injecting *foxj1a* mRNA together with GFP mRNA, as a lineage tracer, into one-cell stage *aei*$^{-/-}$ mutant embryos. We found that cilia length was rescued in the KV cells that expressed GFP (Fig. 3H). Although in the *aei*$^{-/-}$ mutant KV cells the average cilia length was 2.25 μm, in the rescued *aei*$^{-/-}$ mutant cells, the average was 4±0.37 μm (s.d.m.) (n=53 cilia/5 embryos; $P<1.0\times10^{-5}$). This experiment confirmed that *foxj1a* functions downstream of DeltaD.

Short cilia generate a weak fluid flow inside the KV

To evaluate the impact that the shorter cilia of *aei*$^{-/-}$ mutants might have on the fluid flow inside the KV, we measured the velocity of the flow in these mutants and compared it with wild-type embryos. For this, we filmed KVs of live embryos and tracked naturally occurring particles that move with the fluid flow (Fig. 4A,A′,B,B′; see Movies 1 and 2 in the supplementary material). This non-invasive method safeguards the epithelium and natural osmotic pressure inside the KV. We showed that in *aei*$^{-/-}$ mutants, velocity of the fluid flow is less than half than that of its wild-type siblings (Fig. 4C; 6.74 μm/s and 16.46 μm/s, respectively; $P<1.5\times10^{-4}$). Importantly, directionality of the flow is only lost in *aei*$^{-/-}$ mutants (Fig. 4B-B′, see Movie 2 in the supplementary material). Loss of directionality could be due to a perturbation in the normal distribution of cilia inside the KV. However, a detailed 3D reconstruction of the spatial distribution of cilia in the KV of *aei*$^{-/-}$ mutants revealed no significant differences when compared with wild-type embryos (Fig. 4D). We thus conclude that the reduced cilia length documented here constitute the most probable cause for the slow and chaotic fluid flow observed in *aei*$^{-/-}$ mutants.

A strong KV fluid flow promotes asymmetric *charon* expression

Charon is a Cerberus/Dan family secreted factor expressed specifically in the cells that line the posterior domain of the KV in a horseshoe shape (Fig. 4H). This protein negatively regulates Nodal signalling by blocking the transfer of Spaw from the KV to the right side of the LPM in zebrafish and medaka (Hashimoto et al., 2004; Hojo et al., 2007). In addition, it has been suggested that *charon* might be a potential Notch signalling target in zebrafish (Gourronc et al., 2007). We confirmed this possibility by injecting *deltaD* or *NICD* mRNA into one-cell stage wild-type embryos, which resulted in clear ectopic expression of *charon* in the KV region (Fig. 4F,G). By contrast, the expression of *charon* in *aei*$^{-/-}$ mutants was severely reduced in 35.4% of the embryos from eight- to 12-somite stage (Fig. 4O,P), whereas in *bea*$^{-/-}$ mutants it was unaffected. Together, these data confirmed that *charon* is a target of the Notch signalling pathway in zebrafish.

In contrast to what has been described (Hashimoto et al., 2004), we found that *charon* expression in a wild-type zebrafish KV is initially symmetric from the five- to seven-somite stage and then becomes clearly asymmetric on the right side from eight-somite stage onwards (Fig. 4H-K). It is still unclear whether the switch to higher levels on the right side corresponds to a downregulation of *charon* levels on the left side or to an upregulation on the right side of the KV. Our results identify *charon* as the first asymmetric gene expressed in the zebrafish KV and provide a better explanation for the mechanism underlying the asymmetric inhibition of Spaw transfer to the right LPM.

As we show that *charon* expression becomes asymmetric after being symmetrically induced (Fig. 4H-K), we asked whether fluid flow in the KV could be the mechanism controlling this switch, as suggested in medaka and in *Xenopus* (Hojo et al., 2007; Schweickert et al., 2010). In contrast to wild-type embryos where there is a clear shift from symmetric to an asymmetric *charon* expression at the eight-somite stage (Fig. 4K), in the *aei*$^{-/-}$ mutants, this shift does not occur (Fig. 4P). In fact, in *aei*$^{-/-}$ mutant embryos where the expression of *charon* was not severely reduced, we could score it as being symmetric in 43.3% and asymmetric in only 21.3% from 8-12 somite stages (Fig. 4L-P). This suggests that the slower fluid flow in *aei*$^{-/-}$ mutants characterized above is inefficient to promote the asymmetry switch of *charon* expression in KV cells.

Having shown that DeltaD regulates *charon* transcription (Fig. 4L-P), we could hypothesize that the inability to shift to the asymmetric *charon* expression observed in *aei*$^{-/-}$ mutants may be caused by a transcriptional defect and not by the slow flow. To investigate the impact of KV fluid flow on *charon* expression in a transcription competent context, we repeated the experiment in *left-right dynein1* (*lrd1*) morphants. These morphants have a very reduced or absent flow (Essner et al., 2005) and show no problems in *charon* transcription (Gourronc et al., 2007). We injected *lrd1-MO* into wild-type embryos and scored *charon* expression in eight- to 12-somite stage embryos. We observed that in *lrd1* morphants the asymmetric shift in *charon* expression does not occur (Fig. 4R), strengthening the idea that the fluid

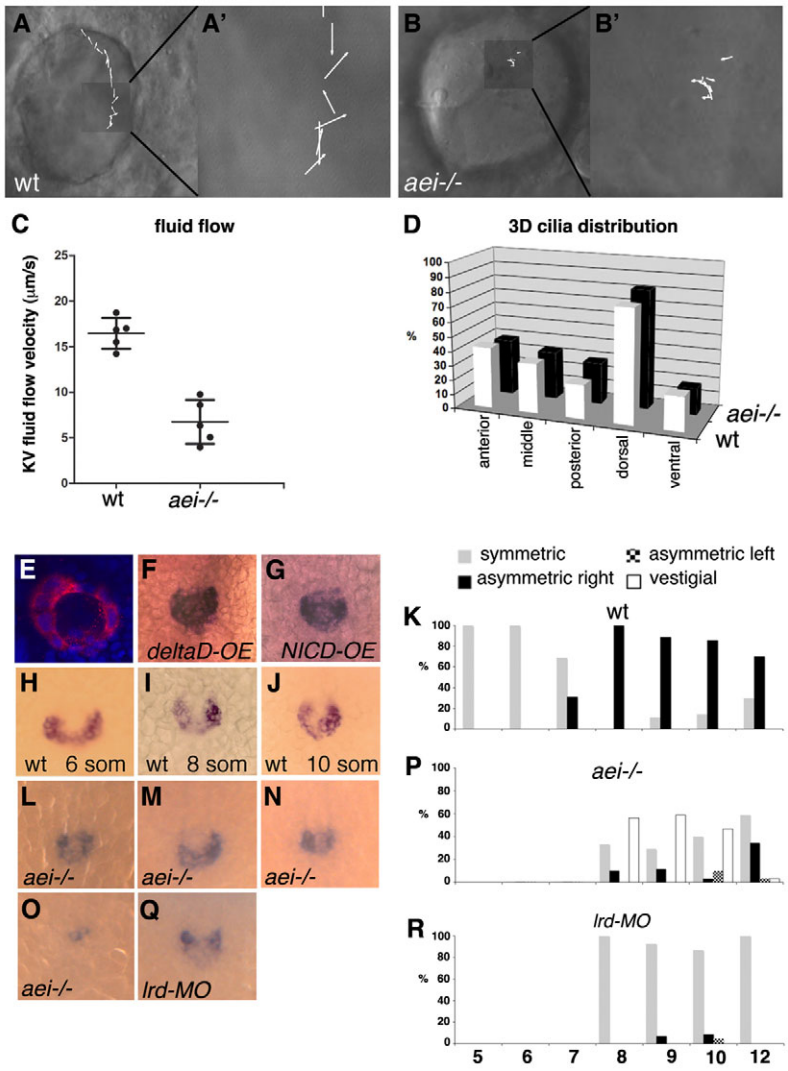

Fig. 4. Short cilia reduce fluid flow inside Kupffer´s vesicle and compromise *charon* asymmetric expression. (**A-B'**) Still images from wild-type siblings (A) and *aei*$^{-/-}$ mutant embryos (B) taken from Movies 1 and 2, respectively, in the supplementary material. Inserts A′ and B′ show vectors representing the fluid flow velocity and direction in each experimental situation. (**C**) Quantification of the average fluid flow velocity in wild type (n=5, 16.46±1.69 μm/s) and in *aei*$^{-/-}$ mutants (n=5, 6.74±2.41 μm/s). (**D**) Percentage of cilia in different regions of Kupffer´s vesicle (anterior, middle, posterior, dorsal and ventral) in wild-type (n=19) and *aei*$^{-/-}$ mutant embryos (n=14). (**E**) A 10-somite stage embryo showing nuclei stained with DAPI in blue and *charon* mRNA cytoplasmic localization in the epithelial cells that surround the lumen of Kupffer´s vesicle. (**F**,**G**) Expression pattern of *charon* in Kupffer´s vesicle of embryos overexpressing *deltaD* (F) and NICD (G). (**H-J**) *charon* expression at Kupffer´s vesicle is symmetric at the six-somite stage (H) and is asymmetric at the eight- and ten-somite stages (I,J). (**K**) Percentage of symmetric versus asymmetric *charon* expression in Kupffer´s vesicle in wild-type embryos from five- to 12-somite stages (n=18 for each stage). (**L-O**) Range of expression patterns of *charon* in Kupffer´s vesicle of *aei*$^{-/-}$ mutant embryos; *charon* expression may be symmetric (L), asymmetric with stronger expression on the right (M), asymmetric with stronger expression on the left (N) or reduced (O). (**P**) Percentages of the different *charon* expression patterns in Kupffer´s vesicle in *aei*$^{-/-}$ mutant embryos from the eight- to 12-somite stages (n=34 on average for each stage). (**Q**) *charon* expression pattern in Kupffer´s vesicle of one representative *lrd1* morphant. (**R**) Percentage of symmetric versus asymmetric *charon* expression in Kupffer´s vesicle of *lrd1* morphants from the eight- to 12-somite stages (n=27 on average for each stage).

flow inside the KV is crucial for inducing asymmetric *charon* expression. Our results, together with those obtained in other species, clearly show that *charon* transcription is sensitive to fluid flow. Therefore, we suggest that *charon* and its homologues may be candidates for flow-sensing genes in the KV/GRP/node environment.

DISCUSSION

The involvement of Notch signalling in the establishment of the left-right axis is evolutionary conserved among vertebrates. However, there are differences in the mode of action of this molecular signalling pathway between mammals and fish. In the mouse, the analysis of Notch pathway mutants reveals that *nodal* induction in the murine node is impaired (Krebs et al., 2003; Przemeck et al., 2003; Raya et al., 2003; Takeuchi et al., 2007), whereas the expression of the secreted Nodal antagonist *cerl2* does not seem to be affected (Krebs et al., 2003; Przemeck et al., 2003; Raya et al., 2003; Takeuchi et al., 2007). By contrast, the expression of *spaw* is normal in zebrafish embryos treated with DAPT (a Notch signalling inhibitor) but the expression of the secreted Nodal antagonist *charon* is severely affected in the KV (Gourronc et al., 2007). Using a genetic approach, we were able to confirm and extend these pharmacological results to conclude that the relevant Notch ligand for *charon* transcription in zebrafish is DeltaD. Therefore, Notch signalling in these two organisms targets the transcription of different genes: *nodal* in the mouse and *charon* in the zebrafish.

In the mouse node, the symmetric expression of *nodal*, induced by Notch signalling, and that of *cerl2*, induced by an unknown mechanism, later becomes asymmetric. *nodal* levels become higher on the left side, whereas *cerl2* levels are higher on the right side of the node (Marques et al., 2004). In contrast to what happens in the mouse, there was no evidence for an asymmetric *spaw* or *charon* expression in the zebrafish KV. In our study, we discovered a sharp transition from a symmetric to an asymmetric expression of *charon* at the eight-somite stage in the KV, with higher levels of expression on the right side. This finding strengthens the evolutionary conserved feature of *charon* expression because this gene, and its homologues, are asymmetrically expressed on the right side in medaka KV (Hojo et al., 2007), *Xenopus* gastrocoel roof plate (GRP) (Schweickert et al., 2010) and mouse node (Marques et al., 2004). The mechanism that triggers the left bias of *nodal* expression in the murine node and the right bias of *charon* and *coco* expression on the right side in fish KV and *Xenopus* GRP remains poorly understood.

There is increasing evidence in these organisms that the extracellular fluid flow generated by motile cilia present in the node/KV/GRP is essential to establish the LR asymmetries in the

LPM. Therefore, this directional fluid flow is a good candidate to trigger the initial asymmetric expression at the node/KV/GRP (Hamada, 2008). We discovered that in *aei*$^{-/-}$ mutants, the switch in *charon* expression does not occur, possibly as a consequence of the slower fluid flow generated by the short motile cilia. In agreement with the possibility that the dynamics of the fluid flow promote a switch in gene expression in the node/KV/GRP are the phenotypes described for the *axonemal dynein* morphants in fish and *Xenopus* and the mouse mutants *iv* and *inv*. In medaka and as shown here in zebrafish embryos, the right bias in *charon* expression is no longer detected when fluid flow is abolished by the knockdown of *lrd1* (Hojo et al., 2007) (Fig. 4Q,R). In *Xenopus*, *coco* is no longer downregulated on the left side of the GRP in the absence of flow (Schweickert et al., 2010). In the *iv* mouse mutant, where cilia are immotile and no nodal flow is produced, the expression of *nodal* in the node becomes randomized (Okada et al., 1999). In addition, in the *inv* mouse mutant, where the flow is slow and turbulent, the expression of *nodal* is mostly symmetric in the node (Lowe et al., 1996; Okada et al., 1999; Oki et al., 2009).

Although no asymmetric *charon* expression had been detected before in zebrafish, asymmetric Charon function was suggested to be responsible for inhibiting the transference of Spaw from the KV domain to the right LPM (Hashimoto et al., 2004). However, it should be emphasized that in wild-type embryos, *charon* is also expressed on the left side of the KV and *spaw* can still be transferred to the left LPM. This suggests that it is not the absence of *charon* transcripts that allow Spaw transfer to the left LPM but the relative levels of *charon* expression between left and right sides. Thus, we reason that Spaw is transferred to the left LPM because the levels of *charon* transcripts are lower on the left side of the KV in a wild-type embryo.

Applying the same reasoning to the *aei*$^{-/-}$ mutants, we propose that the severely reduced *charon* expression observed in 35.4% of the embryos (Fig. 4O,P) could correspond to: (1) no differences in the relative levels of *charon* [and therefore *spaw* is bilateraly transferred to the LPM as observed in 20% of *aei*$^{-/-}$ embryos (Fig. 1A)]; or (2) undetected small differences in *charon* expression that lead to a weak bilateral situation described as a *spaw* left anterior domain with bilateral posterior domains as observed in 15% of *aei*$^{-/-}$ embryos (Fig. 1A). In 43.3% of *aei*$^{-/-}$ mutants, *charon* expression is largely symmetric as visualized by in situ hybridization (Fig. 4L,P). In this situation, we cannot rule out that a biased difference between the left and the right side of *charon* transcripts in *aei*$^{-/-}$ mutants is still present as most embryos express left-sided *spaw* in the LPM (Fig. 1A). A clear asymmetric *charon* expression pattern on the right side of the KV (Fig. 4M) was observed in 18.3% of *aei*$^{-/-}$ embryos, resulting in left-sided *spaw* expression in the LPM (Fig. 1A). A few embryos (3%) expressed *charon* more strongly on the left side of the KV (Fig. 4N), matching the equivalent percentage of right-sided *spaw* in the LPM (Fig. 1A).

In summary, we showed that shorter cilia present in *aei*$^{-/-}$ mutants produce a slower fluid flow that leads to abnormal LR *charon* levels at the KV, which compromises the maintenance of *spaw* expression in the posterior domain of the left LPM. We show that in the same embryos where we observed a premature downregulation of *spaw*, we also see a reduced *lefty1* expression in the posterior midline domain. We thus propose that this gap in *lefty1* expression contributes, together with abnormal posterior *pitx2* expression, to the gut laterality defects without affecting heart laterality. This phenotype is clinically relevant as there are reports on individuals with primary ciliary dyskinesia that develop situs inversus abdominalis with no heart laterality defects (Fliegauf et al., 2007).

To our knowledge, Notch signalling is the first pathway that can both increase or decrease ciliary length, upon upregulation or downregulation, respectively. By contrast, FGF signalling has only been involved in shortening cilia length, (Hong and Dawid, 2009; Yamauchi et al., 2009). Our experiments identify *foxj1a*, the master motile ciliogenic transcription factor (Yu et al., 2008) as being downstream of DeltaD because it successfully rescued cilia length in *aei*$^{-/-}$ mutants in a cell-autonomous manner. These observations perhaps indicate that the motile cilia programme controlled by *foxj1a*, involves not only the transcription of motility genes such as *dnah9* and *wdr78* (Yu et al., 2008) but may also transcribe genes important for cilia growth yet to be discovered.

A systematic analysis of the experimental conditions where short and long cilia are generated by modulating the Notch activity will provide a framework to determine relevant ciliary length control genes. This will certainly bring new insights into how cilia/flagella length is regulated and may provide ways to increase ciliary length that could ultimately be used to treat ciliopathies often characterized by short cilia (Wemmer and Marshall, 2007).

Acknowledgements

We thank J. Lewis and S. Holley for fixed *aei*^{tr233} and *bea*^{tit446} mutant embryos, respectively; A. Oates for *Su(H)1+2-MO*; and S. Roy, W. Norton, S. Wilson, J. Yost, C.-P. Heisenberg, M. Hibi and J. Lewis for in situ probes. We are grateful to A. T. Tavares, J. Regan, D. Henrique, A. Jacinto, M. Godinho Ferreira, M. Bettencourt-Dias, J. Lewis, R. Monteiro, S. Marques and the Saúde labaoratory for comments on the manuscript; and to Lara Carvalho and the zebrafish facility team for excellent fish husbandry. S.S.L. and R.L. were supported by FCT fellowships (SFRH/BPD/34822/2007 and SFRH/BD/24861/2005). L.S. was supported by two FCT grants (PTDC/SAU-OBD/71596/2006 and PTDC/SAU-OBD/64628/2006).

Competing interests statement

The authors declare no competing financial interests.

Supplementary material

Supplementary material for this article is available at
http://dev.biologists.org/lookup/suppl/doi:10.1242/dev.054452/-/DC1

References

Amack, J. and Yost, H. (2004). The T box transcription factor No Tail in ciliated cells controls zebrafish left-right asymmetry. *Curr. Biol.* **14**, 685-690.

Amack, J., Wang, X. and Yost, H. (2007). Two T-box genes play independent and cooperative roles to regulate morphogenesis of ciliated Kupffer's vesicle in zebrafish. In *Dev. Biol.* **310**, 196-210.

Bisgrove, B., Snarr, B., Emrazian, A. and Yost, H. (2005). Polaris and Polycystin-2 in dorsal forerunner cells and Kupffer's vesicle are required for specification of the zebrafish left-right axis. *Dev. Biol.* **15**, 274-288.

Chin, A. J., Tsang, M. and Weinberg, E. S. (2000). Heart and gut chiralities are controlled independently from initial heart position in the developing zebrafish. *Dev. Biol.* **227**, 403-421.

Collignon, J., Varlet, I. and Robertson, E. J. (1996). Relationship between asymmetric nodal expression and the direction of embryonic turning. *Nature* **381**, 155-158.

Echeverri, K. and Oates, A. (2007). Coordination of symmetric cyclic gene expression during somitogenesis by Suppressor of Hairless involves regulation of retinoic acid catabolism. *Dev. Biol.* **301**, 388-403.

Essner, J. J., Amack, J. D., Nyholm, M. K., Harris, E. B. and Yost, H. J. (2005). Kupffer's vesicle is a ciliated organ of asymmetry in the zebrafish embryo that initiates left-right development of the brain, heart and gut. *Development* **132**, 1247-1260.

Fior, R. and Henrique, D. (2009). "Notch-Off": a perspective on the termination of Notch signalling. *Int. J. Dev. Biol.* **53**,1379-1384. Review.

Fliegauf, M., Benzing, T. and Omran, H. (2007). When cilia go bad: cilia defects and ciliopathies. *Nat. Rev. Mol. Cell Biol.* **8**, 880-893.

Gerdes, J. M., Davis, E. E. and Katsanis, N. (2009). The vertebrate primary cilium in development, homeostasis, and disease. *Cell* **137**, 32-45.

Gourronc, F., Ahmad, N., Nedza, N., Eggleston, T. and Rebagliati, M. (2007). Nodal activity around Kupffer's vesicle depends on the T-box transcription factors notail and spadetail and on notch signaling. *Dev. Dyn.* **236**, 2131-2146.
Hamada, H. (2008). Breakthroughs and future challenges in left-right patterning. *Dev. Growth Differ.* **5**, S71-S78.
Hamada, H., Meno, C., Watanabe, D. and Saijoh, Y. (2002). Establishment of vertebrate left-right asymmetry. *Nat. Rev. Genet.* **3**, 103-113.
Hashimoto, H., Rebagliati, M., Ahmad, N., Muraoka, O., Kurokawa, T., Hibi, M. and Suzuki, T. (2004). The Cerberus/Dan-family protein Charon is a negative regulator of Nodal signaling during left-right patterning in zebrafish. *Development* **131**, 1741-1753.
Hojo, M., Takashima, S., Kobayashi, D., Sumeragi, A., Shimada, A., Tsukahara, T., Yokoi, H., Narita, T., Jindo, T., Kage, T. et al. (2007). Right-elevated expression of charon is regulated by fluid flow in medaka Kupffer's vesicle. *Dev. Growth Differ.* **49**, 395-405.
Holley, S. A., Geisler, R. and Nüsslein-Volhard, C. (2000). Control of her1 expression during zebrafish somitogenesis by a delta-dependent oscillator and an independent wave-front activity. *Genes Dev.* **14**, 1678-1690.
Hong, S. K. and Dawid, I. B. (2009). FGF-dependent left-right asymmetry patterning in zebrafish is mediated by Ier2 and Fibp1. *Proc. Natl. Acad. Sci. USA* **106**, 2230-2235.
Hsiao, C. D., You, M. S., Guh, Y. J., Ma, M., Jiang, Y. J. and Hwang, P. P. (2007). A positive regulatory loop between foxi3a and foxi3b is essential for specification and differentiation of zebrafish epidermal ionocytes. *PLoS ONE* **2**, e302.
Kimmel, C. B., Ballard, W. W., Kimmel, S. R., Ullmann, B. and Schilling, T. F. (1995). Stages of embryonic development of the zebrafish. *Dev. Dyn.* **203**, 253-310.
Kramer-Zucker, A., Olale, F., Haycraft, C., Yoder, B., Schier, A. and Drummond, I. (2005). Cilia-driven fluid flow in the zebrafish pronephros, brain and Kupffer's vesicle is required for normal organogenesis. *Development* **132**, 1907-1921.
Krebs, L. T., Iwai, N., Nonaka, S., Welsh, I. C., Lan, Y., Jiang, R., Saijoh, Y., O'Brien, T. P., Hamada, H. and Gridley, T. (2003). Notch signaling regulates left-right asymmetry determination by inducing Nodal expression. *Genes Dev.* **17**, 1207-1212.
Latimer, A. J. and Appel, B. (2006). Notch signaling regulates midline cell specification and proliferation in zebrafish. *Dev. Biol.* **298**, 392-402.
Levin, M. and Palmer, A. R. (2007). Left-right patterning from the inside out: widespread evidence for intracellular control. *BioEssays* **29**, 271-287.
Lin, X. and Xu, X. (2009). Distinct functions of Wnt/beta-catenin signaling in KV development and cardiac asymmetry. *Development* **136**, 207-217.
Long, S., Ahmad, N. and Rebagliati, M. (2003). The zebrafish nodal-related gene southpaw is required for visceral and diencephalic left-right asymmetry. *Development* **130**, 2303-2316.
Lowe, L. A., Supp, D. M., Sampath, K., Yokoyama, T., Wright, C. V., Potter, S. S., Overbeek, P. and Kuehn, M. R. (1996). Conserved left-right asymmetry of nodal expression and alterations in murine situs inversus. *Nature* **381**, 158-161.
Marques, S., Borges, A. C., Silva, A. C., Freitas, S., Cordenonsi, M. and Belo, J. A. (2004). The activity of the Nodal antagonist Cerl-2 in the mouse node is required for correct L/R body axis. *Genes Dev.* **18**, 2342-2347.
Monteiro, R., van Dinther, M., Bakkers, J., Wilkinson, R., Patient, R., ten Dijke, P. and Mummery, C. (2008). Two novel type II receptors mediate BMP signalling and are required to establish left-right asymmetry in zebrafish. *Dev. Biol.* **315**, 55-71.
Neugebauer, J. M., Amack, J. D., Peterson, A. G., Bisgrove, B. W. and Yost, H. J. (2009). FGF signalling during embryo development regulates cilia length in diverse epithelia. *Nature* **458**, 651-654.
Nonaka, S., Tanaka, Y., Okada, Y., Takeda, S., Harada, A., Kanai, Y., Kido, M. and Hirokawa, N. (1998). Randomization of left-right asymmetry due to loss of nodal cilia generating leftward flow of extraembryonic fluid in mice lacking KIF3B motor protein. *Cell* **95**, 829-837.
Okada, Y., Nonaka, S., Tanaka, Y., Saijoh, Y., Hamada, H. and Hirokawa, N. (1999). Abnormal nodal flow precedes situs inversus in iv and inv mice. *Mol. Cell* **4**, 459-468.
Oki, S., Kitajima, K., Marques, S., Belo, J. A., Yokoyama, T., Hamada, H. and Meno, C. (2009). Reversal of left-right asymmetry induced by aberrant Nodal signaling in the node of mouse embryos. *Development* **136**, 3917-3925.
Przemeck, G. K., Heinzmann, U., Beckers, J. and Hrabé de Angelis, M. (2003). Node and midline defects are associated with left-right development in Delta1 mutant embryos. *Development* **130**, 3-13.
Raya, A., Kawakami, Y., Rodriguez-Esteban, C., Buscher, D., Koth, C. M., Itoh, T., Morita, M., Raya, R. M., Dubova, I., Bessa, J. G. et al. (2003). Notch activity induces Nodal expression and mediates the establishment of left-right asymmetry in vertebrate embryos. *Genes Dev.* **17**, 1213-1218.
Schweickert, A., Vick, P., Getwan, M., Weber, T., Schneider, I., Eberhardt, M., Beyer, T., Pachur, A. and Blum, M. (2010). The nodal inhibitor Coco is a critical target of leftward flow in Xenopus. *Curr. Biol*. Epub ahead of print.
Stubbs, J. L., Oishi, I., Izpisúa Belmonte, J. C. and Kintner, C. (2008). The forkhead protein Foxj1 specifies node-like cilia in Xenopus and zebrafish embryos. *Nat. Genet.* **40**, 1454-1460.
Supp, D. M., Brueckner, M., Kuehn, M. R., Witte, D. P., Lowe, L. A., McGrath, J., Corrales, J. and Potter, S. S. (1999). Targeted deletion of the ATP binding domain of left-right dynein confirms its role in specifying development of left-right asymmetries. *Development* **126**, 5495-5504.
Takeuchi, J., Lickert, H., Bisgrove, B., Sun, X., Yamamoto, M., Chawengsaksophak, K., Hamada, H., Yost, H., Rossant, J. and Bruneau, B. (2007). Baf60c is a nuclear Notch signaling component required for the establishment of left-right asymmetry. *Proc. Natl. Acad. Sci. USA* **104**, 846-851.
Takke, C. and Campos-Ortega, J. A. (1999). her1, a zebrafish pair-rule like gene, acts downstream of notch signalling to control somite development. *Development* **126**, 3005-3014.
Takke, C., Dornseifer, P., van Weizsäcker, E. and Campos-Ortega, J. A. (1999). her4, a zebrafish homologue of the Drosophila neurogenic gene E(spl), is a target of NOTCH signalling. *Development* **126**, 1811-1821.
Thisse, C. and Thisse, B. (2008). High-resolution in situ hybridization to whole-mount zebrafish embryos. *Nat. Protoc.* **3**, 59-69.
Wang, X. and Yost, H. J. (2008). Initiation and propagation of posterior to anterior (PA) waves in zebrafish left-right development. *Dev. Dyn.* **237**, 3640-3647.
Wemmer, K. A. and Marshall, W. F. (2007). Flagellar length control in chlamydomonas-paradigm for organelle size regulation. *Int. Rev. Cytol.* **260**, 175-212.
Yamauchi, H., Miyakawa, N., Miyake, A. and Itoh, N. (2009). Fgf4 is required for left-right patterning of visceral organs in zebrafish. *Dev. Biol*. **332**, 177-185.
Yu, X., Ng, C. P., Habacher, H. and Roy, S. (2008). Foxj1 transcription factors are master regulators of the motile ciliogenic program. *Nat. Genet.* **40**, 1445-1453.

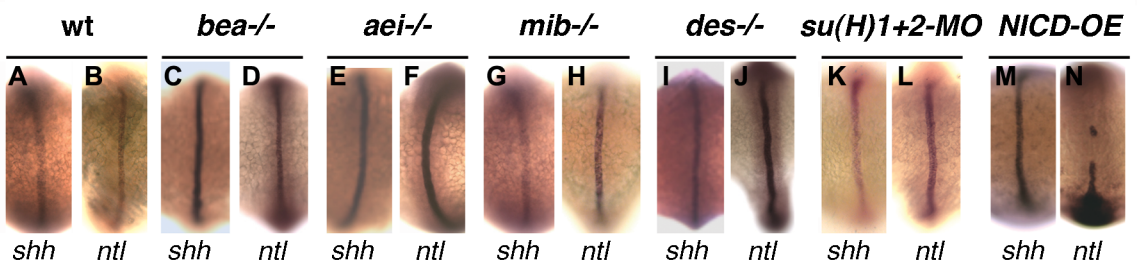
wt
bea-/-
aei-/-
mib-/-
des-/-
su(H)1+2-MO
NICD-OE
A
B
C
D
E
F
G
H
I
J
K
L
M
N
shh
ntl
shh
ntl
shh
ntl
shh
ntl
shh
ntl
shh
ntl
shh
ntl